Pathogenic CD4+ T cells recognizing an unstable peptide of insulin are directly recruited into islets bypassing local lymph nodes

James F. Mohan,[1] Boris Calderon,[1] Mark S. Anderson,[2] and Emil R. Unanue[1]

[1]Department of Pathology and Immunology, Washington University School of Medicine, St. Louis, MO 63110
[2]Diabetes Center, University of California at San Francisco, San Francisco, CA 94115

In the nonobese diabetic mouse, a predominant component of the autoreactive CD4+ T cell repertoire is directed against the B:9–23 segment of the insulin B chain. Previous studies established that the majority of insulin-reactive T cells specifically recognize a weak peptide-MHC binding register within the B:9–23 segment, that to the 12–20 register. These T cells are uniquely stimulated when the B:9–23 peptide, but not the insulin protein, is offered to antigen presenting cells (APCs). Here, we report on a T cell receptor (TCR) transgenic mouse (8F10) that offers important new insights into the biology of these unconventional T cells. Many of the 8F10 CD4+ T cells escaped negative selection and were highly pathogenic. The T cells were directly recruited into islets of Langerhans, where they established contact with resident intra-islet APCs. Immunogenic insulin had to be presented in order for the T cells to localize and cause disease. These T cells bypassed an initial priming stage in the pancreatic lymph node thought to precede islet T cell entry. 8F10 T cells induced the production of antiinsulin antibodies and islets contained immunoglobulin (IgG) deposited on β cells and along the vessel walls.

CORRESPONDENCE
Emil R. Unanue:
unanue@wustl.edu

Abbreviations used: ILN, inguinal LN; LTβR, lymphotoxin β receptor; NOD, nonobese diabetic; PLN, pancreatic LN; T reg cell, regulatory T cell.

The development of autoimmune diabetes in both humans and nonobese diabetic (NOD) mice is highly influenced by specific alleles of the class II MHC genes: HLA-DQ2 and HLA-DQ8 in humans and I-A^{g7} in mice (Acha-Orbea and McDevitt, 1987; Cucca et al., 2001). CD4+ T cells are essential in initiating the autoimmune response and, consequently, much emphasis has been placed on deciphering the relevant self-peptides recognized by these cells driving the development of diabetes (Anderson and Bluestone, 2005).

The work of many laboratories has emphasized the importance of insulin as a critical target of the immune response for the development of autoimmune diabetes (Zhang et al., 2008). Extensive analysis of the T cell response directed against insulin has highlighted an immunodominant segment of the insulin B chain, the B:9-23 (SHLVEALYLVCGERG) peptide (Wegmann et al., 1994a,1994b; Daniel et al., 1995; Abiru et al., 2001; Halbout et al., 2002). CD4+ T cells recognizing B:9-23 are detected within the infiltrated islets of prediabetic mice and antigenic masking of this epitope via mutation or tolerogenic expression in APCs diminished islet autoimmunity, signifying the essential role recognition of the B:9-23 epitope in the development of diabetes (French et al., 1997; Jaeckel et al., 2004; Nakayama et al., 2005). These studies and others convincingly show that insulin is among the foremost targets in NOD diabetes, and its recognition by CD4+ T cells likely initiates a cascade of downstream events driving both the amplification and diversification of the autoimmune response, ultimately resulting in the complete destruction of β cells (Nakayama et al., 2007; Krishnamurthy et al., 2008). As a result, much importance has been placed on understanding

J.F. Mohan and B. Calderon contributed equally to this paper.

The Rockefeller University Press $30.00
J. Exp. Med. 2013 Vol. 210 No. 11 2403-2414
www.jem.org/cgi/doi/10.1084/jem.20130582

the precise details involved in the recognition of the B:9-23 peptide by the immune system, particularly its binding interactions with I-A^{g7} and the nature of the self-reactive T cells that recognize this peptide MHC complex (Abiru et al., 2000; Yu et al., 2000; Levisetti et al., 2007; Crawford et al., 2011; Mohan et al., 2011).

Recently, we described a unique set of diabetogenic insulin-reactive CD4$^+$ T cells that constitute the major component of the T cell repertoire recognizing the B:9-23 peptide (Mohan et al., 2010, 2011; Mohan and Unanue, 2012). Unlike conventional T cells, these T cells specifically recognized exogenous insulin peptides offered to the APCs, but were incapable of recognizing the same peptide generated from processing of the insulin protein by the APC. The conventional T cells, referred to as type A, represented a very small minority (<1%) of the T cells recognizing the B:9-23 peptide. The unconventional T cells, referred to as type B, were abundant (>99% of the T cells recognizing this peptide) in the periphery of NOD mice, indicating that they might be impervious to negative selection in the thymus during development. A single amino acid shift of the B:9-23 peptide segment bound within the groove of I-A^{g7} decisively explained the discordant reactivities between type A and B T cells (Mohan et al., 2011). Type A T cells recognized the 13–21 segment (SHL**EALYVLVCG*E***RG [sequence in bold, the critical P9 residue in bold and italic]) of the B:9-23 peptide bound to I-A^{g7}. In contrast, type B T cells recognized the 12–20 segment of the peptide (SHL**VEALYLVCG***E*RG [sequence in bold, the critical P9 residue in bold and italic]) bound to I-A^{g7}. The 13–21 register (type A) interacts more favorably with I-A^{g7}, whereas the 12–20 register (type B) is largely unstable and rapidly dissociates from I-A^{g7}. Importantly, free peptides from insulin catabolism were identified in β cell secretory granules and in the islet APCs, explaining the presentation of the 12–20 register to the type B T cells (Mohan et al., 2010). It is therefore highly plausible that the binding features and lack of presentation of the 12–20 register after processing of insulin protein explain why type B T cells are capable of escaping thymic selection.

Understanding the biology of these type B T cells that recognize the weak binding register of the B:9-23 peptide, only presented by APC from preformed peptides, requires a TCR transgenic mouse. Here, we report on the generation of a type B TCR transgenic (8F10) mouse specific for the 12–20 segment of the insulin B chain and show that these T cells escape negative selection in the thymus, are spontaneously recruited to the islets by intra-islet APCs charged with insulin peptide–MHC complexes, induce local inflammation, and are highly pathogenic in the absence of other T cell specificities. The initial activation of these diabetogenic T cells does not appear to occur in the pancreatic LNs (PLNs); instead, they are directly recruited into islets from the vascular network through interactions with resident intra-islet APCs. Their biological properties appear unique and quite different from other insulin T cells described, specifically those with type A reactivity (Du et al., 2006; Jasinski et al., 2006; Fousteri et al., 2012).

RESULTS

Generation of the 8F10 TCR transgenic mouse strain

The 8F10 TCR transgenic mouse was generated using the rearranged TCR α chain (Vα13.3, TRAV5D-4/TRAJ53) and β chain (Vβ8.2, TRBV13-2/TRBD2/TRBJ2-7) cloned from the 8F10 B:9-23 reactive type B T cell. In prior studies, the 8F10 T cell exhibited strong reactivity for APC pulsed with the B:9-23 peptide, while remaining completely unreactive to APC pulsed with the insulin protein. These T cells specifically recognized the type B register 12–20, but completely lacked a response to the type A register 13–21 (Mohan et al., 2010, 2011).

A single founder was obtained with genotypic and phenotypic characteristics indicative of a co-integration of both the TCR α and β chains into a single genetic locus. The total numbers of cells found in the thymus or spleen of 8F10 mice were similar to those found in NOD mice. Flow cytometric analysis of thymus and spleens showed normal T cell development in 8F10 mice (Fig. 1 A). The detection of T cells in the periphery of 8F10 mice implicated their escape from negative selection in the thymus. The ratio of CD4$^+$ versus CD8$^+$ T cells was increased in both the thymus and to a lesser extent in the spleen of 8F10 mice compared with NOD. As expected, the development of CD8$^+$ T cells was impaired in 8F10 mice, seen by their reduced number in thymus and spleen, asserting the notion that the TCR of 8F10 primarily interacts with the MHC class II allele I-A^{g7}.

The vast majority (>95%) of CD4$^+$ cells in 8F10 mice stained positive with the TCR Vβ8.1/8.2 antibody compared with ∼20–25% of T cells in littermate controls (Fig. 1 B). Expression of other TCR Vβ alleles on 8F10 T cells was not observed, thereby confirming allelic exclusion of the endogenous TCR β locus.

Currently, there is no available antibody that recognizes the TCR Vα13.3 allele, so we could not assess the level of surface expression for the transgenic TCR Vα chain. However, despite strong allelic exclusion of the endogenous TCR Vβ locus, many of the peripheral T cells in 8F10 mice exhibited successful rearrangements of endogenous TCR α chains. Staining with an antibody that recognizes the TCR Vα2 allele showed that a subset of 8F10 CD4$^+$ T cells expressed this particular TCR α chain (Fig. 1 B). Other minor populations of 8F10 T cells expressed TCR Vα3.2, TCR Vα3.2, or TCR Vα8.3, pointing to a significant fraction of transgenic T cells expressing additional endogenous TCR α chains. This feature is not unique to the 8F10 strain, as other TCR transgenics expressed functional rearrangements of endogenous TCR α gene products (Zal et al., 1994; Fousteri et al., 2012; Mingueneau et al., 2012). The majority of the splenic CD4$^+$ T cells in 8F10 mice exhibited a naive phenotype, proven by the predominance of CD62L^{hi} CD44^{low} T cells (Fig. 1 C).

To restrict the TCR repertoire, 8F10 mice were crossed onto the *recombinase activating gene 1* (*rag1*)–deficient background. Crossing 8F10 mice onto the *rag1*-deficient background prevented the rearrangement of endogenous TCR α chains, thus ensuring that only the transgenic TCRα/β

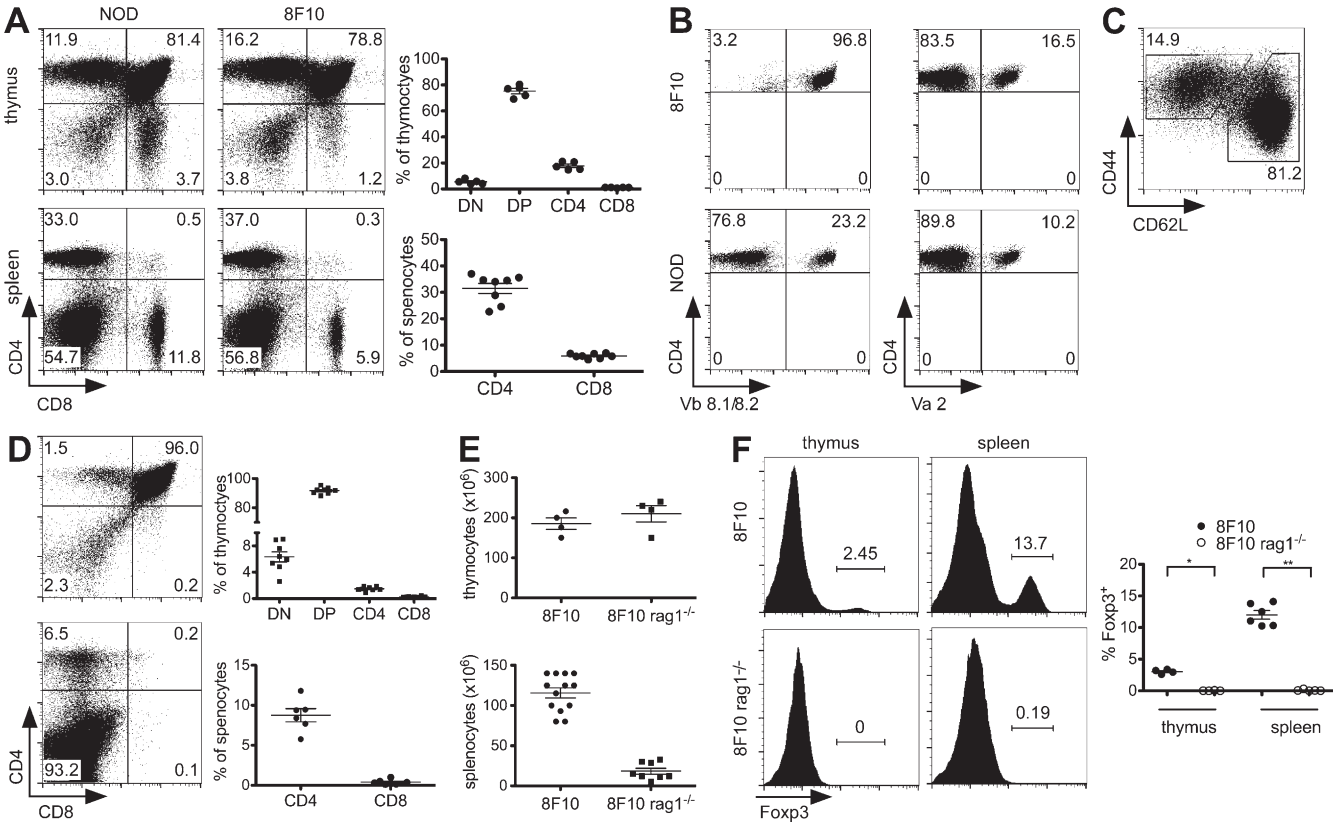

Figure 1. Analysis of 8F10 mice. (A, left) CD4 and CD8 flow cytometric profiles of NOD and 8F10 thymocytes; (right) percentages of cells found among individual 8F10 mice. (B) Cell surface staining of 8F10 and NOD CD4+ splenocytes with anti-TCR Vβ8.1/8.2 (left) or anti-TCR Vα2 (right). (C) Cell surface staining of 8F10 CD4+ splenocytes with anti-CD44 and -CD62L. (D) Thymic (top left) and splenic (bottom left) profiles, and percentages of T cells among individual 8F10 *rag1*$^{-/-}$ mice (right). (E) Absolute number of thymocytes and splenocytes from 8F10 and 8F10 *rag1*$^{-/-}$ mice. (F, left) Foxp3 staining of CD4+ single-positive thymocytes and CD4+ splenocytes of 8F10 and 8F10 *rag1*$^{-/-}$ mice; (right) percentages of Foxp3+ T cells from individual 8F10 and 8F10 *rag1*$^{-/-}$ mice. (A–F) Representative flow cytometry plots and cumulative data from two or more independent experiments (error bars, SEM). Statistical analysis: Mann-Whitney *U* test, (*, $P < 0.05$; **, $P < 0.005$).

chains were expressed. Although the majority of thymocytes in 8F10 *rag1*$^{-/-}$ mice were found in the immature CD4/CD8 double positive population, a small proportion of these cells matured into CD4+ single-positive T cells (Fig. 1 D). Despite the low level of thymic selection in 8F10 *rag1*$^{-/-}$ mice, T cells were present in the periphery and were exclusively CD4+, representing roughly 5–10% of the total splenocytes (Fig. 1 D and Discussion). 8F10 *rag1*$^{-/-}$ mice contained a similar number of thymocytes compared with 8F10 mice, but the number of splenocytes was reduced (Fig. 1 E).

A subset of CD4+ single-positive 8F10 thymocytes expressed the regulatory T cell (T reg) marker Foxp3. In the spleen, a sizable proportion (~10–15%) of CD4+ T cells expressed Foxp3 (Fig. 1 F). Foxp3 expressing T cells were extremely rare, if not entirely absent in both the thymus and periphery of 8F10 *rag1*$^{-/-}$ mice (Fig. 1 F). Thus, the development of T reg cells in 8F10 mice was dependent on the expression of rearranged endogenous TCR α chains, which was prevented when the mice were bred to a *rag1*-deficient background.

Response of 8F10 TCR transgenic T cells to the B:9-23 peptide

CD4+ T cells from the spleen of 8F10 mice responded robustly to the B:9-23 peptide but did not respond to APC pulsed with the insulin protein, confirming the type B reactivity previously reported using the parental T cell line (Fig. 2 A). As the B:9-23 peptide binds in multiple overlapping registers to the I-A^{g7} molecule, we next examined their register reactivity using nested register peptides, each of which contained a single binding register present within the B:9-23 peptide (Mohan et al., 2011). As expected, these T cells responded robustly to the weaker MHC binding B:12-20 register, poorly to the stronger MHC binding B:13-21 register and had no response to the very weak MHC binding register B:14-22 reported by others (Crawford et al., 2011) when presented by I-A^{g7} (Fig. 2 B). T cells from 8F10 *rag1*$^{-/-}$ mice behaved in a similar manner, responding robustly to the B:9-23 peptide and the 12–20 register but poorly to insulin and the 13–21 register (Fig. 2, C and D). T cells from 8F10 *rag1*$^{-/-}$ mice also recognized a nested 12–21 peptide, containing the minimal sequence of both registers in tandem recognized by both type A and B

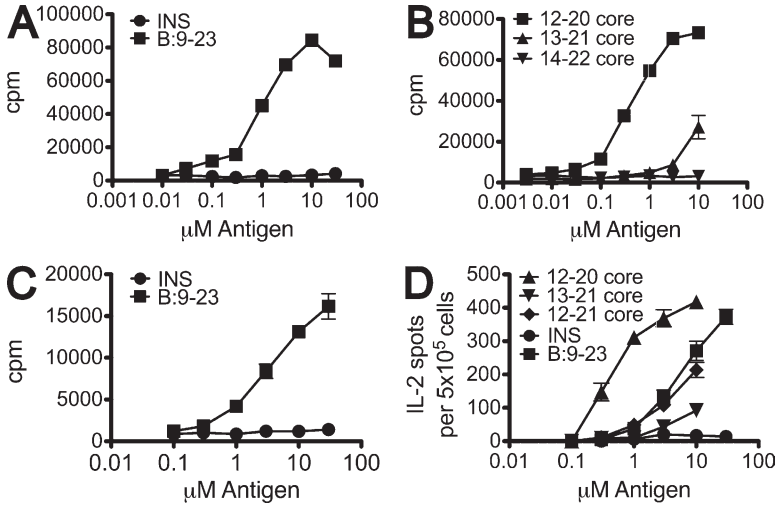

Figure 2. Reactivity of 8F10 CD4+ T cells. (A) Primary proliferation of isolated 8F10 CD4+ T cells in response to B:9-23 peptide and insulin protein presented by CD11c+ DCs. (B) Primary proliferation of isolated 8F10 CD4+ T cells in response to nested register peptides (core peptides) containing a single register of the B:9-23 peptide presented by CD11c+ DCs. (C) Primary proliferation of splenocytes isolated from 8F10 *rag1*$^{-/-}$ mice incubated with insulin or B:9-23 peptide. (D) Enzyme-linked immunospot (ELISPOT) assay of IL-2 secretion by splenocytes isolated from 8F10 *rag1*$^{-/-}$ mice pulsed with the B:9-23 peptide, insulin protein, or nested register peptides (core peptides). (A–D) Data representative of two independent experiments (error bars, SEM).

insulin-reactive T cells. The reactivity to the nested 12–21 peptide was similar to the response observed for the B:9-23 peptide, both of which were weaker than the response observed for the nested 12–20 peptide (Fig. 2 D). When APCs are offered the B:9-23 and the nested 12–21 peptide they bind to I-A^{g7} in multiple independent registers, thus partially diminishing the response compared with the nested 12–20 peptide that specifically binds in the sole register, recognized by the 8F10 TCR. As expected, in six different trials islet APCs presented to 8F10 as shown previously for all insulin-reactive T cells (Mohan et al., 2010).

T cell entrance into islets

Immunofluorescence microscopy of isolated islets showed the presence of 8F10 T cells within the islets at 3 wk of age, the first point examined. At 5–10 wk of age, ∼60% of the islets contained anywhere from a single T cell to >50 per islet (Fig. 3 A). Older mice exhibited even further infiltration, with roughly 90% of islets containing T cells and an overall greater mean T cell burden per islet (Fig. 3 B). A phenotypic analysis of the intra-islet T cells is described in the next section. Induction of VCAM-1 in intra-islet vessels was also observed in the infiltrated islets of 8F10 mice (Fig. 3, A and B). VCAM-1 is an adhesion molecule not expressed in resting islets, but rapidly up-regulated upon entrance of diabetogenic T cells (Calderon et al., 2011a). Many of the T cells found inside the islets were in direct contact with the resident intra-islet APCs (Fig. 3 C). We previously reported that the resident intra-islet APCs were heavily charged with B:9-23 peptide–MHC complexes and stimulated B:9-23 reactive T cell hybridomas ex vivo (Calderon et al., 2008; Mohan et al., 2010). These findings are in line with the notion that the resident intra-islet APCs provide the local stimulatory signal within the islets to infiltrating T cells.

IgG deposition was detected in many islets in 8F10 mice, suggesting the presence of islet autoantibodies (Fig. 3 D). IgG was found on the surface of the majority of islet cells in a speckled pattern and, intriguingly, in discrete deposits along the islet blood vessel walls (Fig. 3 D). In experiments in which nonspecific IgG was injected into mice, we did not observed localization in islets. The sera of 8–12-wk-old 8F10 mice contained antibodies to native insulin, which were completely blocked by the addition of soluble insulin in the assay (Fig. 3 E). The antisera did not react with denatured insulin, B:9-23 peptide, or with Nit-1 insulinoma cell membranes (Levisetti et al., 2003). Sera from NOD mice did not show detectable levels of anti-insulin antibodies in our assay at this time. These observations suggest that antiinsulin antibodies are made inside islets and form immune complexes with insulin. The number of B cells inside the islets during the early 8–12-wk period at the time that antibodies were found was about one per islet (in 155 islets examined). B cells were found in only 10% of the islets of non-diabetic NOD mice at the 8–12-wk period; this limited number has made it difficult at this point to establish their reactivity (Carrero et al., 2013). Further studies aimed at characterizing their specificity are currently in progress.

To gain a better understanding of the importance of antigen specificity in the recruitment of T cells into the islets, we transplanted bone marrow cells of 8F10 *rag1*$^{-/-}$ mice into lethally irradiated B16:A-dKO mice (B16A). These mice express a single insulin gene with a tyrosine-to-alanine mutation at the 16th residue of the B:9-23 peptide and do not develop diabetes (Nakayama et al., 2005). This mutation completely abrogates the antigenicity of the B:9-23 peptide for both type A and B CD4+ T cells (Abiru et al., 2000, Mohan et al., 2010). 8F10 localized to islets of NOD mice, whereas localization was minimal in B16A mice. Unmanipulated B16A mice showed minimal localization into islets when compared with regular NOD mice (Fig. 3 F). Furthermore, diabetes developed in irradiated NOD mice transplanted with bone marrow of 8F10 *rag1*$^{-/-}$ but not in B16A mice that received the same cells (Fig. 3 F). To note, but not shown in Fig. 3, is that a different CD4+ T cell, the BDC 2.5, induced diabetes when adoptively transferred into irradiated B16A mice: 6/6 were diabetic within 8 d after the transfer of 4 × 10^6 activated T cells.

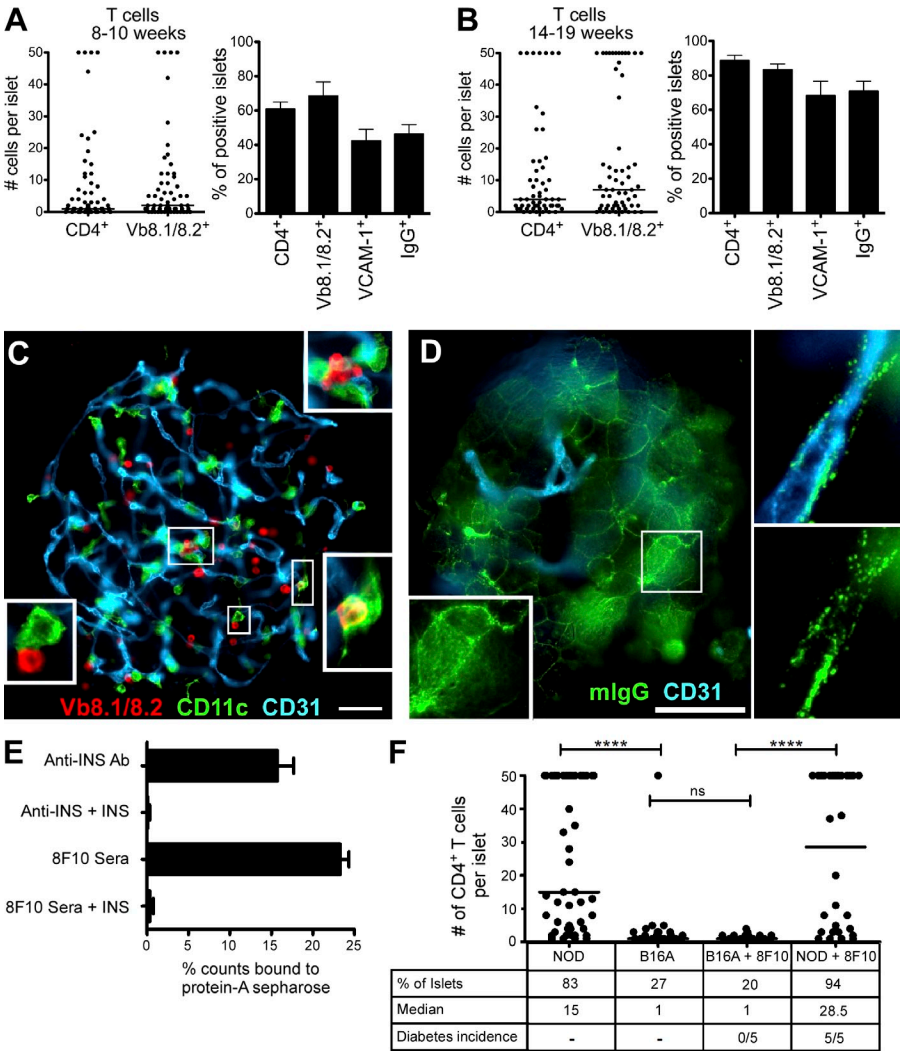

Figure 3. Recruitment of 8F10 T cells to islets and islet reactivity. Islet cytology evaluation of 8F10 female mice at 8–10 (A) or 14–19 (B) wk of age. (A and B, left) Number of T cells (CD4+ or Vα8.1/8.2+) per individual islet; bars indicate the median number of T cells per islet. (A and B, right) Percentage of islets positive for CD4+ T cells, Vβ8.1/8.2+ T cells, VCAM-1+ expression on vessels and mouse IgG+ deposition from pooled islets (n = 5 mice per group) and 100 islets screened for each marker. (C) Representative immunofluorescence image of an islet from A showing T cells by Vα8.1/8.2+ staining. Insets show T cell–APC contacts. (D) Representative islet from A showing mouse IgG deposition on the β cells (left). Inset shows IgG+ deposition on β cell membrane. (right) IgG+ deposition found along intra-islet vessels from A. (E) Radiolabeled I-125 insulin response of antiinsulin antibody or 8F10 mouse sera (8–12 wk) in the presence or absence of competing insulin (INS). (F) Unmanipulated controls (NOD and B16A) and bone marrow chimeric mice (8F10/B16A and 8F10/NOD) indicating the number of CD4+ T cells and the percentages of islets containing T cells; bars indicate the median number of T cells per islet. Indicated is diabetes incidence of irradiated B16A and NOD recipients reconstituted with 8F10 *rag1*$^{-/-}$ bone marrow. (A–F) All data representative of two or more independent experiments (error bars, SEM). Bars, 50 µm. Statistical analysis Mann-Whitney *U* test (ns, not significant; ****, $P < 0.0001$).

Therefore, the localization of 8F10 T cells in islets is antigen specific and requires the recognition of insulin peptides. The mechanisms of 8F10 T cell entry are currently under investigation, but preliminary results indicate that the entry does not appear to involve chemokines, as treatment with pertussis toxin did not block their entrance. In conclusion, type B reactive 8F10 T cells specifically infiltrated islets, initiated local reactivity, and induced conformational antiinsulin autoantibodies analogous to those often found in the serum of type 1 diabetics and human patients at high risk.

Pathogenicity of 8F10 T cells

The development of histopathological lesions in the islets of 8F10 mice is shown in Fig. 4 A. Lymphocytic infiltration was evident at 3 wk of age and increased as the mice aged. By 12 wk of age, extensive infiltration was observed in the majority of islets (Fig. 4 A). Islet infiltration was heterogeneous, some islets exhibited a complete elimination of β cells, and some exhibited mild intra-insulitis, while many others exhibited strong periinsulitic lesions with unaffected β cells (Fig. 4 B). A subset (~20% of islets) showed no signs of lymphocytic infiltration by histological examination. The heterogeneous nature in islet pathology may well be related to the variations in the number of resident intra-islet APC, which can vary from a single APC to >10 APCs per islet (Calderon et al, 2008, 2012).

8F10 mice did not develop diabetes even when followed for >8 mo, despite the inflammation observed in the majority of islets. The finding of inflammation in which the periinsulitic lesion predominates rather than a more destructive insulitis was indicative of a level of suppression controlling β cell destruction. In support of this notion, 23% (±5%) of the T cells isolated from islets were Foxp3+ (Fig. 4 C). The majority of T cells in the islets, 93.2% (±3%), expressed low levels of CD62L, indicating an activation status. In contrast, the LN T cells expressed high levels of CD62L, indicating a clear difference between those in LNs (naive status) and those inside islets (Fig. 4 C).

Strikingly, when the 8F10 mice were crossed onto a *rag1*-deficient background to exclude both endogenous TCR α chain rearrangements and the development of Foxp3 T reg cells, all 8F10 *rag1*$^{-/-}$ mice rapidly developed diabetes, with the majority of mice succumbing to disease at 4–7 wk of age (Fig. 4 D and 4E). The pathological finding was restricted to the islets,

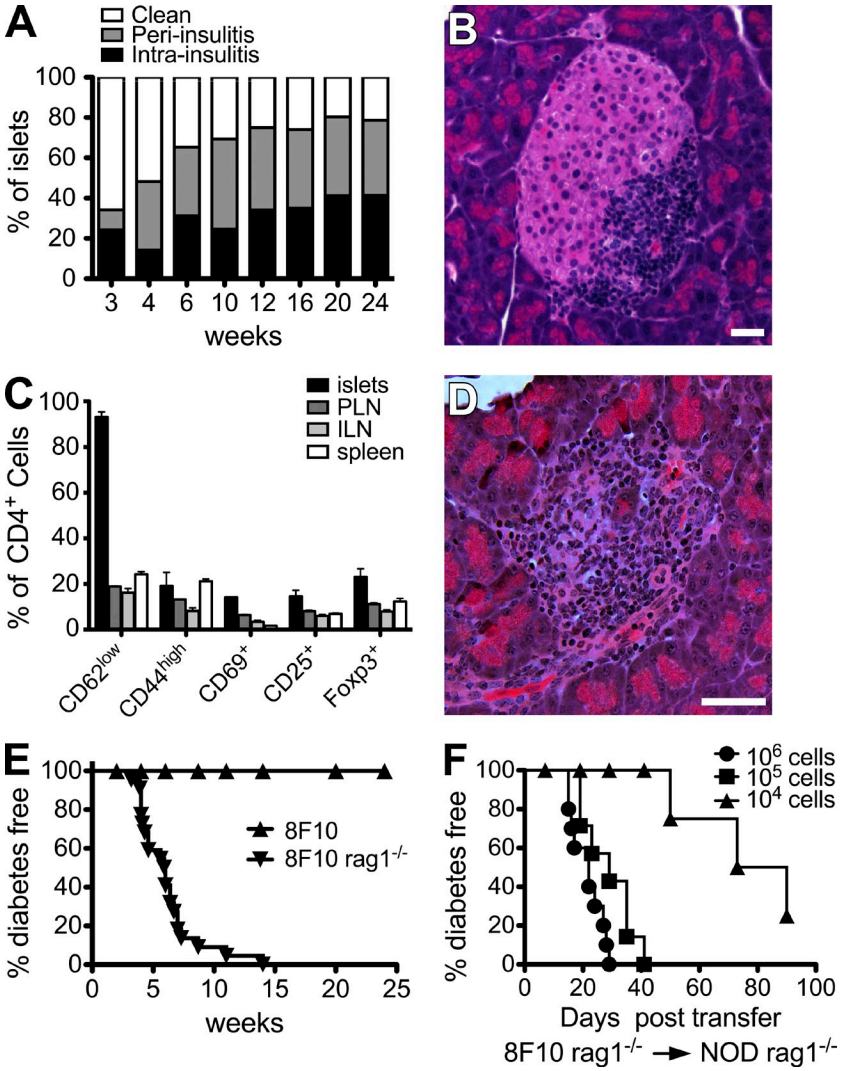

Figure 4. 8F10 T cells are specifically recruited to the islets and are highly pathogenic. (A) Insulitis scoring of pancreatic sections from 8F10 mice stained with hematoxylin and eosin (n = 4–7 mice per age group). (B) Hematoxylin and eosin–stained pancreatic section from a representative islet of a 6-wk-old 8F10 mouse showing the periinsulitic lesion. (C) Flow cytometry analysis of islet-infiltrating 8F10 CD4+ T cells and T cells from other anatomical locations (PLN, ILN [inguinal LN], and spleen) in 10-wk-old 8F10 mice. Dispersed islets were pooled from 4 mice. (D) Pancreatic section from a diabetic 5-wk-old 8F10 *rag1*$^{-/-}$ mouse showing an islet with destructive insulitis. (E) Spontaneous diabetes incidence in 8F10 (n = 60) and 8F10 *rag1*$^{-/-}$ mice (n = 22). (F) Adoptive transfer of splenocytes from 8F10 *rag1*$^{-/-}$ mice into NOD *rag1*$^{-/-}$ recipient mice (10^6, n = 10; 10^5, n = 8; 10^4, n = 4). (A–F) Cumulative data pooled from at least two independent experiments (error bars, SEM).

and no pathology was found in the ovaries, adrenals, thyroid, liver, or kidneys. Thus, there was a dramatic shift in the pathogenicity of these T cells in 8F10 *rag1*$^{-/-}$ mice. Splenocytes from diabetic 8F10 *rag1*$^{-/-}$ mice were highly pathogenic when transferred into adult NOD *rag1*$^{-/-}$ recipients at low numbers of T cells (10^4 splenocytes contained ~500 to 1,000 CD4+ T cells; Fig. 4 F). These findings with 8F10 are compatible with earlier studies involving the BDC 2.5 TCR transgenic mouse extensively studied by the Mathis-Benoist laboratory, which also exhibited a level of regulation and greatly enhanced pathogenicity when bred to a *rag1*-deficient background (Gonzalez et al., 2001; Chen et al., 2005).

In conclusion, 8F10 T cells can initiate and potently cause diabetes in the absence of any other T cell specificities and T reg cells. It is important to note that the diabetes incidence in these mice, whose T cells specifically recognize the weaker of the two registers present in the B:9-23 peptide, is considerably more rapid and penetrant when compared with other reported B:9-23 TCR transgenic strains (Du et al., 2006; Jasinski et al., 2006).

8F10 T cells do not require PLNs

A longstanding tenet in autoimmunity is that LNs draining the target tissue are important in the priming of autoreactive lymphocytes. Strong evidence indicates that the initiation of diabetogenesis commences with the priming of islet reactive T cells in the PLNs before their recruitment to the islets (Höglund et al., 1999; Calderon and Unanue, 2012). Indeed, NOD mice lacking the PLN did not develop diabetes and for the most part were devoid of overt islet infiltration (Gagnerault et al., 2002; Levisetti et al., 2004). Furthermore, findings of two diabetogenic TCR transgenic models, namely BDC 2.5 and 8.3-NOD, representing islet CD4+ and CD8+ T cells, respectively, showed their proliferation in the PLNs from an early age. The results suggest that priming of diabetogenic T cells in the PLNs precedes the migration of these T cells into the islets (Höglund et al., 1999; Zhang et al., 2002). How exactly the PLN functions in T cell priming and its requirement in localization of T cells to the islets are not entirely known.

Previously, we reported that insulin-reactive T cells recognized endogenous presentation of B:9-23 by resident intra-islet

APCs but not by APCs in the draining PLN (Mohan et al., 2010). These results were unexpected but not entirely conclusive, as ex vivo T cell assays are far less sensitive than those performed in vivo. In light of these issues and the finding of 8F10 T cells in islets from an early age, we tested the role of the PLN in priming of insulin-reactive T cells in vivo. Adoptively transferred, CFSE-labeled 8F10 $CD4^+$ T cells did not proliferate in the PLN of recipient NOD mice that ranged in age from 4 to 13 wk old (Fig. 5, A and B). The lack of proliferation observed with 8F10 T cells in the PLN or other nearby LNs, did not appear to result from active suppression as 8F10 T cells also failed to proliferate in the absence of $CD25^+$ cells (Fig. 5 C). 8F10 T cells proliferated vigorously in vitro in the presence of APC and antigen (Fig. 5 D). Finally, despite the lack of reactivity in the PLN, 8F10 T cells were recruited to the islets and proliferated locally, most likely triggered by the resident intra-islet APC (Fig. 5 E). In agreement with others, we found that the BDC2.5 TCR transgenic T cells proliferated in the PLN (Fig. 5 F). The results summarized in Fig. 5 G, indicate that unlike other diabetogenic T cells, 8F10 T cells are only stimulated directly within the islets and not in the draining PLN.

To study the role of the PLN we generated 8F10 mice that lacked most LNs by treating pregnant mice with a soluble lymphotoxin β-receptor (LtβR-Ig) decoy protein. This treatment inhibits the development of most LNs in progeny and results in mice devoid of LNs which remain absent for their lifespan (Rennert et al., 1996, 1998; Mandik-Nayak et al., 2002; Levisetti et al., 2004). 8F10 mice exposed to soluble LTβR-Ig in utero (8F10 nodeless) had absent axillary, inguinal LN (ILN), and popliteal LNs, and of particular relevance to this study, they also lacked the PLN. Importantly, 8F10 nodeless mice did not exhibit any discernible differences in the splenic T cell repertoire compared with T cells that developed in 8F10 mice.

Immunofluorescence of isolated islets from 8F10 nodeless mice indicated that a large proportion of islets were infiltrated with T cells by 5 wk of age (Fig. 6 A). The level of islet T cell infiltration in 8F10 nodeless mice was on par with the amount of infiltration observed in normal 8F10 mice (Fig. 6 B). Histological analysis showed mononuclear infiltrates in the islets of 8F10 nodeless mice (Fig. 6 C). Furthermore, 8F10 *rag1*$^{-/-}$ nodeless mice developed diabetes with similar kinetics to 8F10 *rag1*$^{-/-}$ mice (Fig. 6, D and E). Hence, the PLN is dispensable for the recruitment of 8F10 T cells into the islets, and the development of diabetes in 8F10 *rag1*$^{-/-}$ mice does not depend on an initial priming stage in the PLN.

DISCUSSION

In this study, we report on the unique biological features of an important set of insulin-reactive $CD4^+$ T cells, those that recognize the weak 12–20 register of the insulin B:9-23 segment.

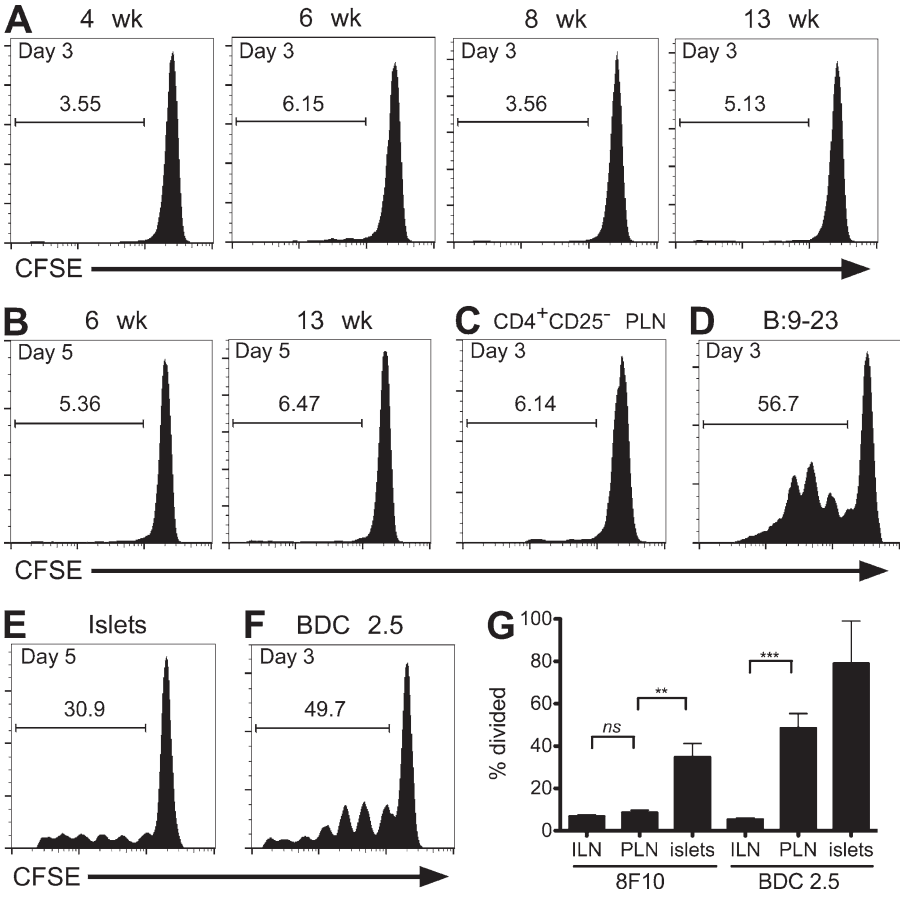

Figure 5. 8F10 T cells are not effectively primed in the PLN. CFSE dilution of 8F10 $CD4^+$ T cells in the PLN of recipient NOD mice of the indicated ages at days 3 (A) and 5 (B) after transfer and analyzed by flow cytometry. (C) CFSE dilution of purified transferred $CD4^+$ $CD25^-$ 8F10 T cells in the PLNs of NOD mice. (D) In vitro CFSE dilution of purified 8F10 $CD4^+$ T cells in the presence of irradiated splenocytes pulsed with B:9-23 peptide. (E) CFSE dilution of 8F10 $CD4^+$ T cells transferred and isolated from the islets of 8-wk-old NOD mice. (F) CFSE dilution of BDC 2.5 $CD4^+$ T cells in the PLN of 8-wk-old NOD mice.(G) Pooled results from multiple experiments depicting percentage of divided 8F10 and BDC 2.5 $CD4^+$ T cells in the ILN, PLN, and islets of NOD recipients. Representative data of at least two independent experiments (A–F) or cumulative data of 2–6 independent experiments (G; error bars, SEM; ns, not significant; **, $P < 0.005$; ***, $P < 0.0005$).

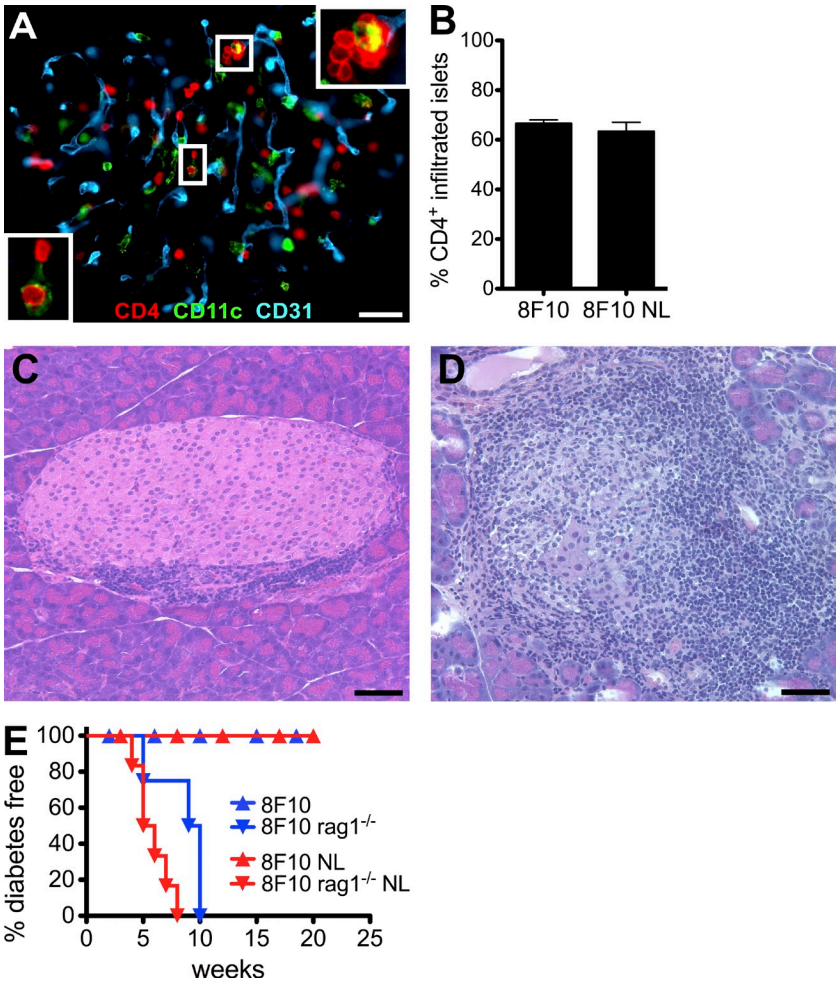

Figure 6. Islet-infiltrating 8F10 T cells do not require priming in the PLN. (A) Immunofluorescence of a representative islet from 5-wk-old 8F10 nodeless mice. Inserts show T cell–APC contacts. (B) Quantitative analysis showing percentage of infiltrating CD4+ T cells in islets of 5-wk-old 8F10 and 8F10 nodeless mice. (C) Hematoxylin and eosin–stained pancreatic section from a 12-wk-old 8F10 nodeless mouse. (D) Hematoxylin and eosin–stained pancreatic section from a 5-wk-old 8F10 *rag1*$^{-/-}$ nodeless diabetic mouse. (E) Spontaneous diabetes incidence of 8F10 (n = 10), 8F10 nodeless (8F10 NL, n = 9), 8F10 *rag1*$^{-/-}$ (8F10 *rag1*$^{-/-}$, n = 4), and 8F10 *rag1*$^{-/-}$ nodeless (8F10 Rag *rag1*$^{-/-}$ NL, n = 6) mice. Representative (A, C, and D) or cumulative (B and E) data pooled from two to three independent experiments. Bars, 50 µm. Error bars, SEM.

The 8F10 T cells: (a) evaded negative selection and peripheralized; (b) entered the islets of Langerhans, where they interacted with resident intra-islet APCs and were pathogenic; (c) did not require priming in the PLN to cause diabetes; and (d) served as helper cells inducing antiinsulin antibodies to native insulin, despite their reactivity to only a preformed peptide segment of the insulin molecule.

These mice provide new insights into the anatomical location where autoreactive T cells recognize insulin. There are four potential anatomical sites for presentation of insulin: (a) centrally by the thymic APC system; (b) by APC of various secondary lymphoid organs; (c) specifically by APC in the PLN; and (d) by resident APCs found in the islets of Langerhans. First, the thymus epithelium is known to express insulin under the control of AIRE to purge the T cell repertoire of insulin-reactive cells (Anderson et al., 2002). Thymic insulin expression likely accounts for the strong selection against type A B:9-23 reactive T cells. Under normal conditions, however, T cells that recognize the unstable 12–20 register akin to 8F10 T cells, are not interacting or interacting poorly with insulin-expressing APC in the thymus for several complementary reasons: expression of insulin by epithelial cells is too low; processing of insulin in the thymus is different from that in β cells in which the generation of the mature hormone from the prohormone is subjected to a specific proteolytic program; and lastly, the biochemical features of the 12–20 register, namely, its poor binding to I-A^{g7} reduces the chances for efficient presentation. In toto, it is likely that the combination of these features result in the inability to purge 8F10 T cells, despite their inherent pathogenicity.

Concerning the sites of presentation in peripheral sites, either splenic and/or blood-borne APCs could potentially take up and present insulin molecules circulating through the bloodstream. Systemic presentation has not been observed, likely because of the low concentration of insulin in blood coupled with the weak interaction of B:9-23 with I-A^{g7}. The third location, the PLN which drains the pancreas, represents an important site, having been shown to prime diabetogenic T cells and as necessary for the development of diabetes (Höglund et al., 1999; Gagnerault et al., 2002; Turley et al., 2003; Levisetti et al., 2004;). Surprisingly, insulin was presented either very weakly or not at all in the PLNs. The biochemical features of this peptide, namely the short lifespan of the register bound to I-A^{g7}, likely explains the lack of detectable presentation of B:9-23 in the PLN.

8F10 T cells were recruited to the islets from an early age, indicating that either denatured insulin or free B chain peptides

were naturally and constitutively presented there. Indeed, we previously reported on the finding of insulin peptides within most of the resident intra-islet APCs, a finding compatible with the present identification of 8F10 T cells establishing intimate contacts with the resident intra-islet APCs. The abundant concentration of insulin in β cells combined with the existence of preformed insulin peptides and the constant local sampling and presentation by resident intra-islet APCs outweigh the poor biochemical properties of this register and allows for efficient presentation (Mohan et al., 2010, 2011). An important new finding concerns the requirement for recognition of immunogenic insulin in islets for localization of 8F10 T cells as exemplified in their absence in B16A mice. The finding denotes immunological specificity for the localization of the diabetogenic T cells. In previous studies, we indicated that the localization of specific diabetogenic T cells did not require chemokine responses (Calderon et al., 2011a). Intra-islet APCs are closely associated with the islet vasculature and extend dendrites through the fenestrated endothelium into the lumen of the islet capillaries (Calderon et al., 2011b). Although not conclusive, it is likely that these dendrites, protruding into the local bloodstream and highly charged with B:9-23 peptide–MHC, can actively recruit insulin-reactive T cells directly from the adjacent bloodstream into the islets.

An important new finding is that 8F10 T cells migrated into the islets even though they had not been activated in the PLN and caused diabetes. These findings place a qualification on the role of the PLN. It raises important issues concerning the interaction between insulin-reactive T cells, believed to be among the earliest infiltrating immune cells, and other islet-reactive $CD4^+$ and $CD8^+$ T cells in which the PLN is an integral site of activation. Our findings that very few T cells were found in the islets of the B16A mice is another argument for insulin T cells driving the initiation of diabetes. Moreover, does the recruitment of insulin-reactive T cells directly into the islets influence levels of islet antigen presentation in the PLN? It is conceivable that inflammation induced by early infiltrating, insulin-specific T cells leads to an increase in islet-specific antigen presentation in the PLN, providing both amplification and diversification of the antiislet response necessary for diabetes development. In strong support of this statement are the findings in which a robust $CD8^+$ T cell response in the PLN to a class I MHC epitope derived from the islet-specific glucose-6-phosphate catalytic subunit depended on the prior development of the antiinsulin response (Krishnamurthy et al., 2006).

The emergence of antiinsulin antibodies and the localization in islets was a surprise. A prior study showed that the TCR α chain from insulin-reactive T cells was sufficient to induce circulating insulin autoantibodies (Kobayashi et al., 2008). Our findings indicate that the 8F10 is acting as a helper T cell for B cells that react with native insulin.These findings are intriguing in the perspective of where B cells interact with insulin, that is, whether with circulating insulin, or directly inside the islets. Although we do not have evidence that the IgG in islets or the intra-islet B cells are insulin-reactive, it is tempting to speculate that the islet is a site of B cell selection.

One issue to discuss concerns the lymphopenia observed in the peripheral compartment of 8F10 *rag1*$^{-/-}$ mice. This result was somewhat unexpected because prior studies have shown that B:9-23-reactive type B T cells did not appear to be under selective pressure in thymus (Mohan et al., 2010, 2011). Generally, it has been assumed that lymphopenia observed in the periphery of TCR transgenics on *rag1*-deficient backgrounds was indicative of negative selection against the TCR of investigation. Although this explanation may be valid in certain instances for TCR transgenic models, it should be noted that this is not always the case. Contrary to this notion, a recent study convincingly shows that a highly restricted monoclonal TCR expression profile in the thymus, particularly on the NOD background, can result in insufficient positive selection, thus also augmenting the ability of TCR transgenic T cells to mature and peripheralize (Mingueneau et al., 2012). Specifically, early expression of TCR transgenes leads to overseeding of the double-positive thymocyte compartment in NOD mice, generating heightened competition for positive selection niches, and thereby reducing the likelihood that many of these developing T cells will be effectively positively selected by a limited pool of selecting ligands. In agreement with this model, our study found ample rearrangement of endogenous TCRα chains in 8F10 mice and an abundant pool of double-positive thymocytes in 8F10 *rag1*$^{-/-}$ mice, suggesting similar mechanisms may be involved. Whether insufficient positive selection can explain the low number of $CD4^+$ T cells observed in 8F10 *rag1*$^{-/-}$ mice will require further investigation, but it represents a highly plausible explanation, especially when taken in consideration with our previous studies showing a lack of negative selection against type B B:9-23-reactive T cells in the polyclonal repertoire of NOD mice (Mohan et al., 2010, 2011).

A final issue to note is that 8F10 *rag1*$^{-/-}$ mice exhibited a much more rapid and penetrant diabetic process compared with two other B:9-23-reactive TCR transgenic strains on *rag1*-deficient backgrounds. One insulin-reactive strain (2H6), presumably with type A reactivity, did not exhibit islet pathology and was shown to have suppressive qualities (Du et al., 2006). The second strain (BDC 12–4.1), created by the Eisenbarth laboratory (Jasinski et al., 2006), was included in our earlier studies of type A and B insulin-reactive T cells. $CD4^+$ T cells from these mice were conclusively shown to exhibit type A reactivity, solely reacting with the stronger 13–21 binding register of the B:9-23 peptide (Mohan et al., 2011). Paradoxically, significantly fewer of the BDC 12–4.1 *rag1*$^{-/-}$ mice developed diabetes, and they contained a sizable population of T reg cells compared with *8F10 rag1*$^{-/-}$ mice (Jasinski et al., 2006; Fousteri et al., 2012). In toto, it suggests that strong selective pressure is being exerted on type A 13–21 reactive T cells, whereas considerably less selective pressure is exerted on T cells recognizing the type B 12–20 register. We speculate that in the naturally arising polyclonal T cell repertoire of NOD mice, selective pressure will eliminate the majority of type A B:9-23 reactive T cells, but the limited number that do escape selection have a much greater likelihood of developing regulatory or anergic phenotypes in the periphery. The

type B–reactive T cells on the other hand, pass through thymic selection with relative ease and potentially represent the majority of true pathogenic insulin-reactive T cells.

In conclusion, it is becoming more evident that insulin-reactive type B T cells represent not only a particularly relevant autoreactive T cell population, but are also central players in the response against B:9-23 during diabetogenesis. Understanding of the pathogenic and/or suppressive capabilities of type A and B subsets independently during the disease process will not only benefit the basic understanding of autoimmunity in NOD mice, but may also aid in the future development of antigen-specific therapies aimed at preventing type 1 diabetes.

MATERIALS AND METHODS

Mice. NOD, NOD.Cg-Tg(TcraBDC2.5,TcrbBDC2.5)1Doi/DoiJ (BDC 2.5), NOD.Cg-Tg(TcraTcrbNY8.3)1Pesa/DvsJ (8.3-NOD), NOD on the *rag1*$^{-/-}$, and NOD.Cg-Tg(Ins2*Y16A)1Ell *Ins1*^{tm1Ija} *Ins2*^{tm1Ija}/GseJ (B16:A-dKO) were obtained from The Jackson Laboratory and maintained in specific pathogen–free conditions. All animal studies were approved by the animal study committee of Washington University.

Generation of 8F10 TCR transgenic mice. To generate the transgenic mice, the TCR α chain (Vα13.3, TRAV5D-4/TRAJ53) and β chain (Vβ8.2, TRBV13-2/TRBD2/TRBJ2-7) sequences were isolated by PCR from cDNA sequences generated from the 8F10 T cell. The TCR α and β chains were cloned into CD2 and CD4 expression vectors, respectively (Zhumabekov et al., 1995; Wang et al., 2001). Linearized TCR α and β expression constructs were co-injected into NOD embryos. Mice were genotyped by PCR with the following primer pairs; TCR α forward 5′-GCAGTCTCCAAAGAATTCGCCACC-3′ and TCR α reverse 5′-CAGTTTGTAATTGCTGCCTCCACT-3′; TCR β forward 5′-ATGCACTGCTGCTATTGCTCAGGA-3′ and TCR β reverse 5′-CCGCTGGCACAGAAGTACACTGAT-3′.

Flow cytometry. Single-cell suspensions isolated from various organs were stained with the following antibodies against CD8, TCR Vβ 8.1/8.2, TCR Vβ 4, TCR Vα 2, and CD62L (BD); CD3e and Foxp3 (eBioscience); and CD4, CD69, and CD44 (BioLegend). Stainings were performed according to the manufacturer's protocol. Flow cytometry samples were collected using a FACSCalibur and FACSCanto II flow cytometers (BD) and analyzed using Flow Jo software (Tree Star).

Islet isolation and handling for immunofluorescence. Islets were isolated with some modifications of the original protocol (Lacy and Kostianovsky, 1967; Salvalaggio et al., 2002; Li et al., 2009). In brief, pancreata were isolated and treated with collagenase, followed by several steps of centrifugation and washing, and finally, islets were picked by hand. Immunofluorescence analysis was performed as previously described (Calderon et al., 2008). Isolated islets maintained on ice were preincubated with 10% Fc block, followed by staining with specific labeled monoclonal antibodies for: anti-CD11c Alexa Fluor 488 (clone N418) and anti-CD4 PE (clone RM4-5; BioLegend); anti-TCR Vβ 8.1/8.2 PE (clone MR5-2; BD); anti-CD31 Alexa Fluor 647 (clone 2B8; provided by S. Bogen, Boston University School of Medicine, Boston, MA); goat anti–mouse IgG (H+L) Alexa Fluor 488 (Life Technologies); and biotinylated anti–VCAM-1 (clone 429; eBioscience). Streptavidin Alexa Fluor 555 (Life Technologies) was used as the secondary reagent. Islets were fixed in 1% paraformaldehyde before epi-illumination microscopic analysis. Percentages of islets with infiltrating T cells, VCAM-1 expression, and IgG deposition were generated by scoring 100 individual purified islets from a pool of five mice per group.

In vitro T cell activation assays. Proliferation of primary 8F10 T cells was performed in triplicate in 96-well round bottom tissue culture plates. 10^5 CD4$^+$ T cells enriched from the splenocytes of 8F10 mice were incubated with 10^5 CD11c$^+$ DC isolated from NOD mice treated with Flt-3L at indicated doses of antigens. Flt-3L treatment was used to increase the yield of DC present in treated mice. Both CD4$^+$ T cells and CD11c$^+$ DC were isolated from spleens of donor mice using standard magnetic cell separation (Miltenyi Biotec). In other assays with 8F10 *rag1*$^{-/-}$ mice, unfractionated splenocytes at a density of 5×10^5 cells per well were used. Proliferation was measured by [3H]thymidine incorporation over the last 24 h of a 72-h culture. ELISPOT assays were performed according to the manufacturer's protocol: 8F10 *rag1*$^{-/-}$ splenocytes were incubated overnight with antigen and analyzed for IL-2 secretion. Insulin was purchased from Sigma-Aldrich. All peptides used in this study were synthesized in the laboratory using standard protocols and were previously described. In brief, nested register peptides, based off the native B:9-23 peptide SHLVEALYLVCGERG, were synthesized with identical artificial flanking residues using the following sequences: 12–20 core, TEG-VEALYLVCG-GGS; 12–21 core, EGVEALYLVCGE-GGS; 13–21 core, TEG-EALYLVCGE-GGS; and 14–22 core; TEG-ALYLVCGER GGS.

In vivo T cell activation assays. Activation of T cells in vivo was performed using a standard adoptive transfer system using CFSE-labeled splenocytes. In brief, splenocytes were dissociated into a single-cell suspension. After RBC lysis, splenocytes were washed two times in PBS and incubated with 1.6-μM CFDA SE (Life Technologies) per 10^7 cells for 10 min at 37°C. Reaction was stopped by adding an equal volume of DMEM + 10% FCS. In other assays CD4$^+$ CD25$^-$ splenic primary T cells were isolated by magnetic cell separation (Miltenyi Biotec) before labeling. After CFSE labeling, $2–5 \times 10^7$ labeled splenocytes or $0.5–1 \times 10^7$ CD4$^+$ CD25$^-$ purified T cells were transferred i.v. into NOD recipients. Inguinal, PLNs, and/or islets were harvested 72 or 120 h after transfer and dissociated into single-cell suspensions. Adoptively transferred CFSE cells were gated either on CD3e$^+$ or CD4$^+$ for 8F10 and BDC 2.5, and by TCR Vβ8.1/8.2$^+$ CFSE$^+$ and TCR Vβ 4$^+$ CFSE$^+$, respectively.

Antiinsulin antibody detection and diabetes monitoring. ^{125}I-labeled insulin was purchased from Perkin Elmer (Cat# NEX420010UC). ^{125}I-insulin (~150,000 cpm) was added to tubes containing sera with or without 10 μg/ml unlabeled insulin as competitor and incubated at 4°C for 72 h. After incubation, 25 μl of 25% Protein-A Sepharose was added and incubated on ice for 1–2 h, shaking periodically. The entire sample was layered over 200 μl of an oil mixture [60% dibutylphthalate (Acros #16660-0010)/40% dioctylphthalate (Acros #11709-0010)] in micro test tubes (Bio-Rad Laboratories). Tubes were spun for 4 min in a Beckman 152 microfuge. After spinning, tubes were cut above the pelleted Sepharose, and both the Sepharose pellet and supernatant were counted in a gamma counter.

LtβR-Ig treatment. Pregnant female breeders used to generate 8F10 and 8F10 *rag1*$^{-/-}$ offspring were treated with soluble LtβR-Ig using a previously established protocol (Rennert et al., 1996). Timed pregnant females were treated i.v. with 200 μg of soluble LtβR-Ig fusion protein on days 14 and 17 of gestation. Progeny used in this study were visually inspected and determined to be devoid of ILNs, PLNs, popliteal LNs, and axillary LNs.

Statistical analysis. Mann–Whitney *U* test was used to determine the level of significant differences between samples and was plotted using GraphPad Prism 5 (GraphPad Software, Inc.).

The authors would like to thank Nigel Killeen for providing TCR transgenic expression plasmids and Jeffrey Browning for providing LtβR-Ig. We gratefully acknowledge Michael White and the staff of our Microinjection Core Facility for their assistance in the generation of 8F10 transgenic mice;, Kathy Frederick for assistance with the mouse lines; and Stephen Ferris, Anthony Vomund, and Javier Carrero for assistance in many of the experiments.

This work was funded by grants AI024742, DK058177, and DK20579 from the National Institutes of Health and grants 1-2010-263 and 17-2012-141 from the Juvenile Diabetes Research Foundation.

The authors have no conflicting financial interests.

Submitted: 19 March 2013
Accepted: 11 September 2013

REFERENCES

Abiru, N., D. Wegmann, E. Kawasaki, P. Gottlieb, E. Simone, and G.S. Eisenbarth. 2000. Dual overlapping peptides recognized by insulin peptide B:9-23 T cell receptor AV13S3 T cell clones of the NOD mouse. *J. Autoimmun.* 14:231–237. http://dx.doi.org/10.1006/jaut.2000.0369

Abiru, N., A.K. Maniatis, L. Yu, D. Miao, H. Moriyama, D. Wegmann, and G.S. Eisenbarth. 2001. Peptide and major histocompatibility complex-specific breaking of humoral tolerance to native insulin with the B9-23 peptide in diabetes-prone and normal mice. *Diabetes.* 50:1274–1281. http://dx.doi.org/10.2337/diabetes.50.6.1274

Acha-Orbea, H., and H.O. McDevitt. 1987. The first external domain of the nonobese diabetic mouse class II I-A beta chain is unique. *Proc. Natl. Acad. Sci. USA.* 84:2435–2439. http://dx.doi.org/10.1073/pnas.84.8.2435

Anderson, M.S., and J.A. Bluestone. 2005. The NOD mouse: a model of immune dysregulation. *Annu. Rev. Immunol.* 23:447–485. http://dx.doi.org/10.1146/annurev.immunol.23.021704.115643

Anderson, M.S., E.S. Venanzi, L. Klein, Z. Chen, S.P. Berzins, S.J. Turley, H. von Boehmer, R. Bronson, A. Dierich, C. Benoist, and D. Mathis. 2002. Projection of an immunological self shadow within the thymus by the aire protein. *Science.* 298:1395–1401. http://dx.doi.org/10.1126/science.1075958

Calderon, B., and E.R. Unanue. 2012. Antigen presentation events in autoimmune diabetes. *Curr. Opin. Immunol.* 24:119–128. http://dx.doi.org/10.1016/j.coi.2011.11.005

Calderon, B., A. Suri, M.J. Miller, and E.R. Unanue. 2008. Dendritic cells in islets of Langerhans constitutively present beta cell-derived peptides bound to their class II MHC molecules. *Proc. Natl. Acad. Sci. USA.* 105:6121–6126. http://dx.doi.org/10.1073/pnas.0801973105

Calderon, B., J.A. Carrero, M.J. Miller, and E.R. Unanue. 2011a. Entry of diabetogenic T cells into islets induces changes that lead to amplification of the cellular response. *Proc. Natl. Acad. Sci. USA.* 108:1567–1572. http://dx.doi.org/10.1073/pnas.1018975108

Calderon, B., J.A. Carrero, M.J. Miller, and E.R. Unanue. 2011b. Cellular and molecular events in the localization of diabetogenic T cells to islets of Langerhans. *Proc. Natl. Acad. Sci. USA.* 108:1561–1566. http://dx.doi.org/10.1073/pnas.1018973108

Carrero, J.A., B. Calderon, F. Towfic, M.N. Artyomov, and E.R. Unanue. 2013. Defining the transcriptional and cellular landscape of type 1 diabetes in the NOD mouse. *PLoS ONE.* 8:e59701. http://dx.doi.org/10.1371/journal.pone.0059701

Chen, Z., A.E. Herman, M. Matos, D. Mathis, and C. Benoist. 2005. Where CD4+CD25+ T reg cells impinge on autoimmune diabetes. *J. Exp. Med.* 202:1387–1397. http://dx.doi.org/10.1084/jem.20051409

Crawford, F., B. Stadinski, N. Jin, A. Michels, M. Nakayama, P. Pratt, P. Marrack, G. Eisenbarth, and J.W. Kappler. 2011. Specificity and detection of insulin-reactive CD4+ T cells in type 1 diabetes in the nonobese diabetic (NOD) mouse. *Proc. Natl. Acad. Sci. USA.* 108:16729–16734. http://dx.doi.org/10.1073/pnas.1113954108

Cucca, F., R. Lampis, M. Congia, E. Angius, S. Nutland, S.C. Bain, A.H. Barnett, and J.A. Todd. 2001. A correlation between the relative predisposition of MHC class II alleles to type 1 diabetes and the structure of their proteins. *Hum. Mol. Genet.* 10:2025–2037. http://dx.doi.org/10.1093/hmg/10.19.2025

Daniel, D., R.G. Gill, N. Schloot, and D. Wegmann. 1995. Epitope specificity, cytokine production profile and diabetogenic activity of insulin-specific T cell clones isolated from NOD mice. *Eur. J. Immunol.* 25:1056–1062. http://dx.doi.org/10.1002/eji.1830250430

Du, W., F.S. Wong, M.O. Li, J. Peng, H. Qi, R.A. Flavell, R. Sherwin, and L. Wen. 2006. TGF-beta signaling is required for the function of insulin-reactive T regulatory cells. *J. Clin. Invest.* 116:1360–1370. http://dx.doi.org/10.1172/JCI27030

Fousteri, G., J. Jasinski, A. Dave, M. Nakayama, P. Pagni, F. Lambolez, T. Juntti, G. Sarikonda, Y. Cheng, M. Croft, et al. 2012. Following the fate of one insulin-reactive CD4 T cell: conversion into Teffs and Tregs in the periphery controls diabetes in NOD mice. *Diabetes.* 61:1169–1179. http://dx.doi.org/10.2337/db11-0671

French, M.B., J. Allison, D.S. Cram, H.E. Thomas, M. Dempsey-Collier, A. Silva, H.M. Georgiou, T.W. Kay, L.C. Harrison, and A.M. Lew. 1997. Transgenic expression of mouse proinsulin II prevents diabetes in nonobese diabetic mice. *Diabetes.* 46:34–39. http://dx.doi.org/10.2337/diab.46.1.34

Gagnerault, M.C., J.J. Luan, C. Lotton, and F. Lepault. 2002. Pancreatic lymph nodes are required for priming of beta cell reactive T cells in NOD mice. *J. Exp. Med.* 196:369–377. http://dx.doi.org/10.1084/jem.20011353

Gonzalez, A., I. Andre-Schmutz, C. Carnaud, D. Mathis, and C. Benoist. 2001. Damage control, rather than unresponsiveness, effected by protective DX5+ T cells in autoimmune diabetes. *Nat. Immunol.* 2:1117–1125. http://dx.doi.org/10.1038/ni738

Halbout, P., J.P. Briand, C. Bécourt, S. Muller, and C. Boitard. 2002. T cell response to preproinsulin I and II in the nonobese diabetic mouse. *J. Immunol.* 169:2436–2443.

Höglund, P., J. Mintern, C. Waltzinger, W. Heath, C. Benoist, and D. Mathis. 1999. Initiation of autoimmune diabetes by developmentally regulated presentation of islet cell antigens in the pancreatic lymph nodes. *J. Exp. Med.* 189:331–339. http://dx.doi.org/10.1084/jem.189.2.331

Jaeckel, E., M.A. Lipes, and H. von Boehmer. 2004. Recessive tolerance to preproinsulin 2 reduces but does not abolish type 1 diabetes. *Nat. Immunol.* 5:1028–1035. http://dx.doi.org/10.1038/ni1120

Jasinski, J.M., L. Yu, M. Nakayama, M.M. Li, M.A. Lipes, G.S. Eisenbarth, and E. Liu. 2006. Transgenic insulin (B:9-23) T-cell receptor mice develop autoimmune diabetes dependent on RAG genotype, H-2g7 homozygosity, and insulin 2 gene knockout. *Diabetes.* 55:1978–1984. http://dx.doi.org/10.2337/db06-0058

Kobayashi, M., J. Jasinski, E. Liu, M. Li, D. Miao, L. Zhang, L. Yu, M. Nakayama, and G.S. Eisenbarth. 2008. Conserved T cell receptor alpha-chain induces insulin autoantibodies. *Proc. Natl. Acad. Sci. USA.* 105:10090–10094. http://dx.doi.org/10.1073/pnas.0801648105

Krishnamurthy, B., N.L. Dudek, M.D. McKenzie, A.W. Purcell, A.G. Brooks, S. Gellert, P.G. Colman, L.C. Harrison, A.M. Lew, H.E. Thomas, and T.W. Kay. 2006. Responses against islet antigens in NOD mice are prevented by tolerance to proinsulin but not IGRP. *J. Clin. Invest.* 116:3258–3265. http://dx.doi.org/10.1172/JCI29602

Krishnamurthy, B., L. Mariana, S.A. Gellert, P.G. Colman, L.C. Harrison, A.M. Lew, P. Santamaria, H.E. Thomas, and T.W. Kay. 2008. Autoimmunity to both proinsulin and IGRP is required for diabetes in nonobese diabetic 8.3 TCR transgenic mice. *J. Immunol.* 180:4458–4464.

Lacy, P.E., and M. Kostianovsky. 1967. Method for the isolation of intact islets of Langerhans from the rat pancreas. *Diabetes.* 16:35–39.

Levisetti, M.G., A. Suri, I. Vidavsky, M.L. Gross, O. Kanagawa, and E.R. Unanue. 2003. Autoantibodies and CD4 T cells target a beta cell retroviral envelope protein in non-obese diabetic mice. *Int. Immunol.* 15:1473–1483. http://dx.doi.org/10.1093/intimm/dxg143

Levisetti, M.G., A. Suri, K. Frederick, and E.R. Unanue. 2004. Absence of lymph nodes in NOD mice treated with lymphotoxin-beta receptor immunoglobulin protects from diabetes. *Diabetes.* 53:3115–3119. http://dx.doi.org/10.2337/diabetes.53.12.3115

Levisetti, M.G., A. Suri, S.J. Petzold, and E.R. Unanue. 2007. The insulin-specific T cells of nonobese diabetic mice recognize a weak MHC-binding segment in more than one form. *J. Immunol.* 178:6051–6057.

Li, D.S., Y.H. Yuan, H.J. Tu, Q.L. Liang, and L.J. Dai. 2009. A protocol for islet isolation from mouse pancreas. *Nat. Protoc.* 4:1649–1652. http://dx.doi.org/10.1038/nprot.2009.150

Mandik-Nayak, L., B.T. Wipke, F.F. Shih, E.R. Unanue, and P.M. Allen. 2002. Despite ubiquitous autoantigen expression, arthritogenic autoantibody response initiates in the local lymph node. *Proc. Natl. Acad. Sci. USA.* 99:14368–14373. http://dx.doi.org/10.1073/pnas.182549099

Mingueneau, M., W. Jiang, M. Feuerer, D. Mathis, and C. Benoist. 2012. Thymic negative selection is functional in NOD mice. *J. Exp. Med.* 209:623–637. http://dx.doi.org/10.1084/jem.20112593

Mohan, J.F., and E.R. Unanue. 2012. Unconventional recognition of peptides by T cells and the implications for autoimmunity. *Nat. Rev. Immunol.* 12:721–728. http://dx.doi.org/10.1038/nri3294

Mohan, J.F., M.G. Levisetti, B. Calderon, J.W. Herzog, S.J. Petzold, and E.R. Unanue. 2010. Unique autoreactive T cells recognize insulin peptides generated within the islets of Langerhans in autoimmune diabetes. *Nat. Immunol.* 11:350–354. http://dx.doi.org/10.1038/ni.1850

Mohan, J.F., S.J. Petzold, and E.R. Unanue. 2011. Register shifting of an insulin peptide-MHC complex allows diabetogenic T cells to escape thymic deletion. *J. Exp. Med.* 208:2375–2383. http://dx.doi.org/10.1084/jem.20111502

Nakayama, M., N. Abiru, H. Moriyama, N. Babaya, E. Liu, D. Miao, L.Yu, D.R. Wegmann, J.C. Hutton, J.F. Elliott, and G.S. Eisenbarth. 2005. Prime role for an insulin epitope in the development of type 1 diabetes in NOD mice. *Nature.* 435:220–223. http://dx.doi.org/10.1038/nature03523

Nakayama, M., J.N. Beilke, J.M. Jasinski, M. Kobayashi, D. Miao, M. Li, M.G. Coulombe, E. Liu, J.F. Elliott, R.G. Gill, and G.S. Eisenbarth. 2007. Priming and effector dependence on insulin B:9-23 peptide in NOD islet autoimmunity. *J. Clin. Invest.* 117:1835–1843. http://dx.doi.org/10.1172/JCI31368

Rennert, P.D., J.L. Browning, R. Mebius, F. Mackay, and P.S. Hochman. 1996. Surface lymphotoxin alpha/beta complex is required for the development of peripheral lymphoid organs. *J. Exp. Med.* 184:1999–2006. http://dx.doi.org/10.1084/jem.184.5.1999

Rennert, P.D., D. James, F. Mackay, J.L. Browning, and P.S. Hochman. 1998. Lymph node genesis is induced by signaling through the lymphotoxin beta receptor. *Immunity.* 9:71–79. http://dx.doi.org/10.1016/S1074-7613(00)80589-0

Salvalaggio, P.R., S. Deng, C.E. Ariyan, I. Millet, W.S. Zawalich, G.P. Basadonna, and D.M. Rothstein. 2002. Islet filtration: a simple and rapid new purification procedure that avoids ficoll and improves islet mass and function. *Transplantation.* 74:877–879. http://dx.doi.org/10.1097/00007890-200209270-00023

Turley, S., L. Poirot, M. Hattori, C. Benoist, and D. Mathis. 2003. Physiological beta cell death triggers priming of self-reactive T cells by dendritic cells in a type-1 diabetes model. *J. Exp. Med.* 198:1527–1537. http://dx.doi.org/10.1084/jem.20030966

Wang, Q., L. Malherbe, D. Zhang, K. Zingler, N. Glaichenhaus, and N. Killeen. 2001. CD4 promotes breadth in the TCR repertoire. *J. Immunol.* 167:4311–4320.

Wegmann, D.R., R.G. Gill, M. Norbury-Glaser, N. Schloot, and D. Daniel. 1994a. Analysis of the spontaneous T cell response to insulin in NOD mice. *J. Autoimmun.* 7:833–843. http://dx.doi.org/10.1006/jaut.1994.1066

Wegmann, D.R., M. Norbury-Glaser, and D. Daniel. 1994b. Insulin-specific T cells are a predominant component of islet infiltrates in pre-diabetic NOD mice. *Eur. J. Immunol.* 24:1853–1857. http://dx.doi.org/10.1002/eji.1830240820

Yu, B., L. Gauthier, D.H. Hausmann, and K.W. Wucherpfennig. 2000. Binding of conserved islet peptides by human and murine MHC class II molecules associated with susceptibility to type I diabetes. *Eur. J. Immunol.* 30:2497–2506. http://dx.doi.org/10.1002/1521-4141(200009)30:9<2497::AID-IMMU2497>3.0.CO;2-J

Zal, T., A. Volkmann, and B. Stockinger. 1994. Mechanisms of tolerance induction in major histocompatibility complex class II-restricted T cells specific for a blood-borne self-antigen. *J. Exp. Med.* 180:2089–2099. http://dx.doi.org/10.1084/jem.180.6.2089

Zhang, Y., B. O'Brien, J. Trudeau, R. Tan, P. Santamaria, and J.P. Dutz. 2002. In situ beta cell death promotes priming of diabetogenic CD8 T lymphocytes. *J. Immunol.* 168:1466–1472.

Zhang, L., M. Nakayama, and G.S. Eisenbarth. 2008. Insulin as an autoantigen in NOD/human diabetes. *Curr. Opin. Immunol.* 20:111–118. http://dx.doi.org/10.1016/j.coi.2007.11.005

Zhumabekov, T., P. Corbella, M. Tolaini, and D. Kioussis. 1995. Improved version of a human CD2 minigene based vector for T cell-specific expression in transgenic mice. *J. Immunol. Methods.* 185:133–140. http://dx.doi.org/10.1016/0022-1759(95)00124-S